



Investigation of aminopyridiopyrazinones as PDE5 inhibitors: Evaluation of modifications to the central ring system

Robert O. Hughes^{a,*}, John K. Walker^a, Jerry W. Cubbage^a, Yvette M. Fobian^a, D. Joseph Rogier^a, Steve E. Heasley^a, Rhadika M. Blevis-Bal^a, Alan G. Benson^a, Dafydd R. Owen^b, E. Jon Jacobsen^a, John N. Freskos^a, John M. Molyneaux^a, David L. Brown^a, William C. Stallings^a, Brad A. Acker^a, Todd M. Maddux^a, Mike B. Tollefson^a, Jennifer M. Williams^a, Joseph B. Moon^a, Brent V. Mischke^a, Jeanne M. Rumsey^a, Yi Zheng^a, Alan MacInnes^a, Brian R. Bond^a, Ying Yu^a

^a Pfizer Global Research and Development, Chesterfield Parkway West, St. Louis, MO 63017, USA

^b Pfizer Global Research and Development, Ramsgate Road, Sandwich, Kent CT13 9NJ, UK

ARTICLE INFO

Article history:

Received 8 May 2009

Revised 28 May 2009

Accepted 1 June 2009

Available online 6 June 2009

Keywords:

PDE5

Pi-pi interaction

Aminopyrazinone

Lead optimization

ABSTRACT

Efforts to improve the potency and physical properties of the aminopyridiopyrazinone class of PDE5 inhibitors through modification of the core ring system are described. Five new ring systems are evaluated and features that impart improved potency and improved solubility are delineated.

© 2009 Elsevier Ltd. All rights reserved.

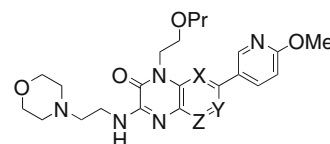
Control of intracellular concentrations of the nucleotide cyclic guanosine monophosphate (cGMP), a second messenger of nitric oxide, is important in regulating vascular tone. Elevation of cGMP levels in vascular smooth muscle cells mediates a reduction in intracellular calcium concentration, resulting in vascular relaxation. Phosphodiesterase type 5 (PDE5) is abundantly expressed in vascular smooth muscle cells, where it specifically hydrolyzes cGMP to the inactive metabolite 5'-GMP. Indeed, in vivo, inhibition of PDE5 results in increases in cGMP levels, leading to vascular relaxation and reduction of systemic blood pressure. Furthermore, pre-clinical and clinical evidence gained with orally active PDE5 inhibitors has revealed benefit in a number of disease indications.¹

As part of our ongoing effort to identify long-acting, potent and selective PDE5 inhibitors, we recently, described the synthesis and initial evaluation of a novel series of aminopyrido[3,2-*b*]pyrazinones (see compound **1** in Table 1).² This series of compounds were derived from a hit uncovered through screening of the Pfizer compound file.

After initial optimization, compounds from this series were discovered which demonstrated good potency against PDE5 and, importantly, selectivity over the closely related isoforms, PDE6 and PDE11. These gains, relative to the initial lead, were obtained

Table 1

Pyrazinone isomers examined as PDE5 inhibitors



Compound	X	Y	Z	Nomenclature
1	N	CH ₂	CH ₂	Northern pyridine
2	CH ₂	CH ₂	CH ₂	Phenyl
3	N	N	CH ₂	Pyrimidine
4	N	CH ₂	N	Pyrazine
5	CH ₂	N	CH ₂	Southeastern pyridine
6	CH ₂	CH ₂	N	Southern pyridine

through modification of the periphery of the pyridopyrazinone core. Generally, however, they came at the expense of physicochemical properties, in particular solubility. Therefore, we sought structural modifications that would yield improved potency without compromising physicochemical properties and the attendant loss in metabolic stability and aqueous solubility. Herein, we describe our evaluation of the core pyrazinone ring system, specifically the nature of the right-hand-side ring.

* Corresponding author. Tel.: +1 636 247 9303.

E-mail address: robert.o.hughes@pfizer.com (R.O. Hughes).

Aminopyrido[3,2-*b*]pyrazinone **1** was previously identified as potent inhibitor of PDE5 ($IC_{50} = 2.9\text{ nM}$). To gain more insight into the structural features that contributed to binding we obtained an X-ray structure of **1** bound to PDE5 at 1.9 Å resolution.³ Examination of **1** in the active site (Fig. 1), led us to reason that the placement of the core pyridyl nitrogen might lead to an unfavorable, repulsive interaction with the sidechain carbonyl, which is held in position via a hydrogen bond network. Thus, removing this interaction, as in **2,5** and **6** (see Table 1), should yield a more potent inhibitor. Furthermore, we noted the potential for edge-to-face (PHE786) and face-to-face (PHE820) pi stacking interactions between PDE5 and the bound inhibitor **1** to significantly contribute to the overall binding energy. We speculated that altering the electronic properties of the core of the molecule might yield compounds with increased potency due to more complementary pi-pi interactions. Wang and Hobza have calculated pi-pi interaction energies for a series of benzene and nitrogen containing heterocyclic dimers and found that the interaction energy of the complex increases as the nitrogen content of the heterocycles increases. Each of these interactions can contribute as much as 4 kcal/mol.⁴ The authors also found that the edge-to-face and the face-to-face interaction energy becomes nearly isoenergetic for the nitrogen containing heterocycles, whereas with the benzene dimer the edge-to-face interaction is more favorable.

Furthermore, we anticipated that lowering the log*D* of the scaffold, for example through incorporation of pyrimidinyl (**3**) or pyrazinyl (**4**) fragments, would have a favorable impact on physicochemical properties. Finally, we hypothesized that the degree of twist in the biaryl axis might correlate with solubility.⁵ Accordingly, we speculated that southern pyridyl isomer **6** would have a higher intrinsic solubility than the relatively flat pyrimidinyl isomer **3**. In order to evaluate these hypotheses, regarding potency and physical properties, and to set the stage for further optimization of the pyrazinone class of PDE5 inhibitors, we targeted the syntheses of additional aminopyrazinone cores, shown in Table 1.

The syntheses of the five novel pyrazinone isomers follow similar reaction sequences which are depicted in Scheme 1. The synthesis of the phenyl and pyrimidinyl isomers commenced with the conversion of **7a,b** to **8a,b** which proceeds smoothly with addition of propoxyethylamine in refluxing ethanol to give the desired amino nitro derivative in 75% yield for the phenyl isomer (**8a**) and

90% for the pyrimidine (**8b**). Reduction of the nitro group to the amine by the action of Raney Ni and hydrogen provided in 40–70% yield the desired diamino isomers **9a,b** with no loss of the halogen. Treatment of **9a,b** with ethyl 2-chloro-2-oxoacetate followed by heating in toluene to affect cyclization gave dione intermediate **10a,b** in 40–70% yield.

Synthesis of the pyrazine isomer, **4**, commenced with addition of propoxyethylamine to 3,5-dibromopyrazin-2-amine in refluxing water to give, regioselectively, **12** in 90% yield. Conversion of this material to the dione, **10c**, was brought about by reaction with oxalyl chloride to give the desired compound in 85% yield.

Synthesis of the southern pyridyl isomer required the selective functionalization of the 3-amino group of 5-bromopyridine-2,3-diamine (**13**). This was realized via a reductive alkylation with 2-propoxyacetaldehyde in the presence of sodium borohydride to give **14** in good yield (75%). Alternately, we could arrive at the same intermediate by selective acylation with 2-propoxyacetyl chloride followed by reduction of the resultant amide with lithium aluminum hydride. Treatment of diamine **14** with ethyl 2-chloro-2-oxoacetate followed by heating gave the desired dione, **10d**, in fair yield (30–50%).

The synthesis of the southeastern isomer **5** began with Boc-protected chloroamino pyridine **15**. Lithiation of **15** with *n*BuLi in the presence of TMEDA followed by quenching with *N*-fluorobenzene-sulfonimide (NFSI) gave the desired fluoropyridine, **16**, in 60% yield. Treatment of **16** with propoxyethyl amine in refluxing EtOH gave the diamino compound **17** in 75% yield. On large scale, these two steps could be conveniently carried out, without purification, in reproducibly good yield. Removal of the Boc group (HCl) followed by treatment with methyl 2-chloro-2-oxoacetate gave the intermediate ester-amide which, upon heating in toluene, was converted to the desired dione **10e** in 85% overall yield.

With the five requisite diones in-hand we undertook the conversion of these intermediates to the elaborated, representative final analogs. Treatment of diones, **10a–e**, with oxalyl chloride in presence of a catalytic amount of DMF gave the derived chloroimides. While isolable, these intermediates were typically used without purification in the subsequent step. Specifically, reaction between the chloroimides, **18a–e**, and aminoethylmorpholine gave **19a–e** cleanly and in good yield. Finally, a Suzuki reaction between the chloro or bromo aminopyrazinones (**19a–e**) and 6-methoxy-pyridin-3-ylboronic acid gave the fully elaborated prototypes, **2–6**, in good overall yield.

Table 2 summarizes the PDE5, PDE6 and PDE11 activity for the prototype members of each of the five new ring systems in comparison to the previously prepared northern pyridyl isomer **1**. We were pleased to find that each of these systems was relatively well tolerated in terms of both potency and selectivity, enhancing our prospects for further optimization. With a PDE5 $IC_{50} = 10.6\text{ nM}$, pyrazine **4** was the least potent of the pyrazinone isomers examined. PDE6 selectivity for this isomer was also modest ($<30\times$). Both phenyl isomer **2** (PDE5 $IC_{50} = 0.9\text{ nM}$) and pyrimidine isomer **3** (PDE5 $IC_{50} = 1.2\text{ nM}$) were approximately equipotent to the northern pyridyl isomer (PDE5 $IC_{50} = 2.9\text{ nM}$) with the phenyl isomer being approximately two-fold more selective over PDE6 than the pyrimidine. Both isomeric pyridines: southern (**6**, PDE5 $IC_{50} = 0.34\text{ nM}$) and southeastern (**5**, PDE5 $IC_{50} = 0.07\text{ nM}$) were found to be significantly more potent than the northern pyridine isomer. As with the northern pyridyl isomer, none of the new core systems demonstrated any appreciable inhibition of PDE11. In this regard, of all the isomers examined pyrazine, **4**, was the least selective at 335-fold.

We rationalized the potency differences between the isomers though a combination of factors. First removal of the lone pair–lone pair repulsion between GLN817's carbonyl and the northern nitrogen of the core (such as **1**, **3**, and **4**) is important for improved

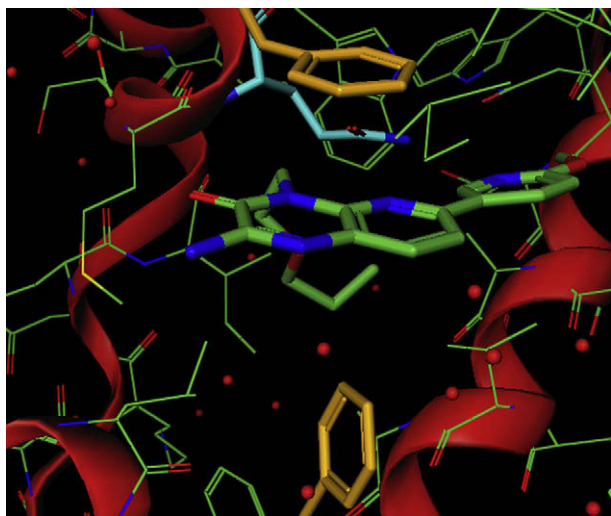
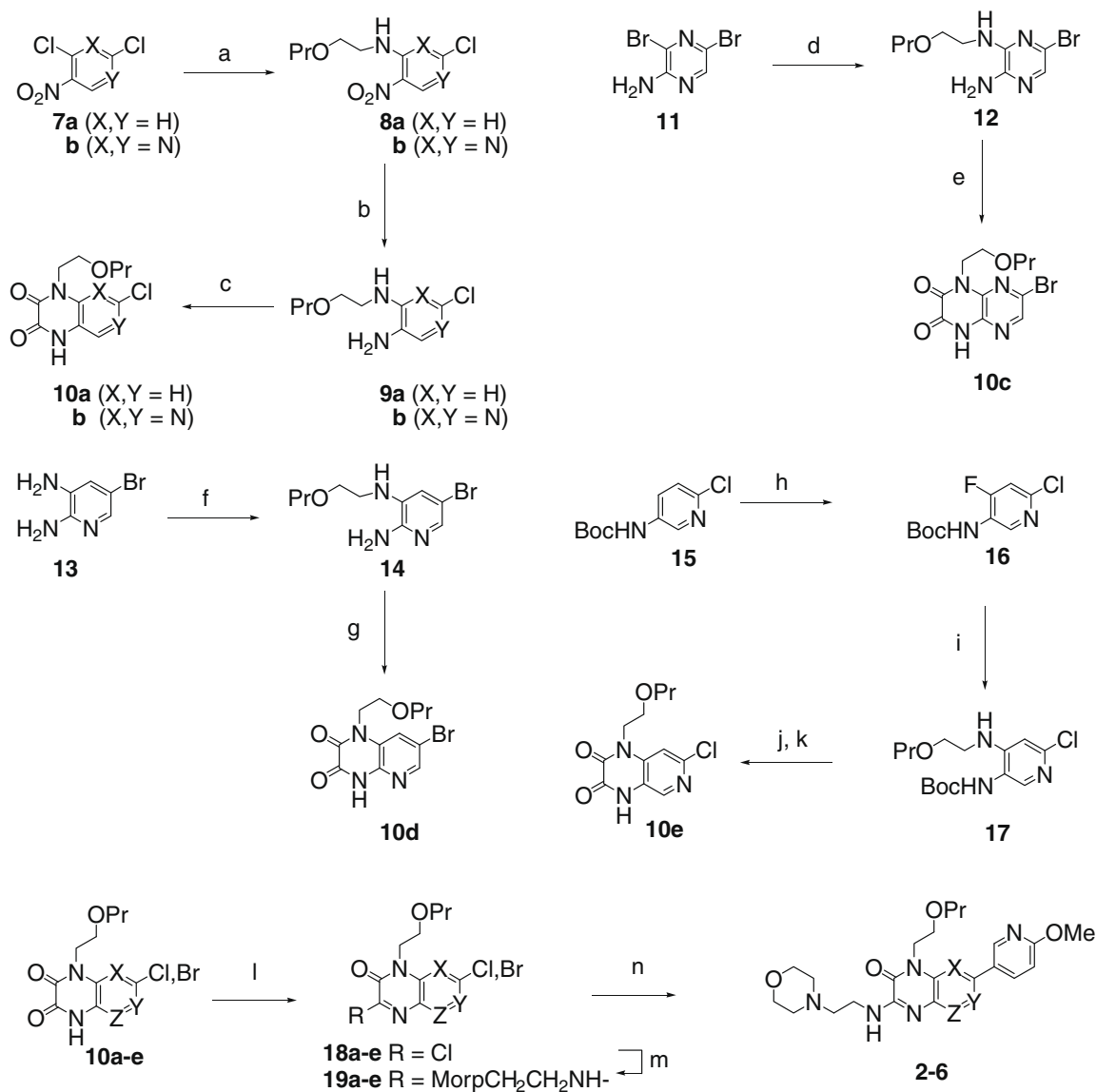


Figure 1. Compound **1** (ethyl morpholine side chain deleted for clarity) bound to PDE5. Highlighted are GLN817 (light blue) and PHE786 (orange) and PHE 820 (orange).



Scheme 1. Synthesis of pyrazinones **2–6**. Reagents and conditions: (a) 2-propoxyethanamine, EtOH, reflux, 12–16 h, 75–90%; (b) Raney Ni/H₂, EtOAc, rt, 16–24 h, 40–70%; (c) ClC(O)CO₂Et, Et₃N, rt to reflux, PhMe, 16–20 h, 40–70%; (d) 2-propoxyethanamine, H₂O, reflux, 12–16 h, 90%; (e) Et₃N, (COCl)₂, CH₂Cl₂, 0 °C to rt, 3 h, 85%; (f) 2-propoxyacetaldehyde, NaBH₄, THF, 4 Å mol sieves, 75%; (g) EtO(CO)(O)Cl, iPr₂NEt, toluene, rt to 90 °C, 2 h, 31–53%; (h) TMEDA, nBuLi, Et₂O, –78 to 10 °C, 2 h; then NFSI, THF –78 to 0 °C, 1 h 60%; (i) 2-propoxyethanamine, EtOH, 75 °C, 12 h 60–80%; (j) 4N HCl, 1,4-dioxane, rt, 1 h; (k) MeOC(O)C(O)Cl, iPr₂NEt, CH₂Cl₂, rt, 4 h; then PhMe, 105 °C, 85% for 2 steps; (l) (COCl)₂, DMF(cat), CH₂Cl₂, rt, 30 min, ~80%; (m) aminoethylmorpholine, Et₃N, CH₂Cl₂, rt, 1 h, 50–90%; (n) 6-methoxyppyridin-3-ylboronic acid, (Ph₃P)₄P (10 mol %), Na₂CO₃, 1,4-dioxane–EtOH, 100 °C, 2 h, 50–85%.

potency. This argument explains why the phenyl isomer **2**, and the southern (**6**) and southeastern (**5**) pyridines are the most potent analogs. Notably, and consistent with the work of Wang and Hobza, both pyridyl isomers are more potent than the phenyl isomer. To further understand the factors governing the differences between these three cores, we examined the representative X-ray structures of the three cores bound to PDE5, but did not observe any movement in either the position of the inhibitor in the binding pocket or the positioning of the PHE residues (not shown). However, since the electronic distribution of the heterocyclic core has changed, the southeastern core likely compliments the pi-pi interaction more favorably than the southern core (Fig. 2). Alternately, the greater aryl-aryl twist in the southern and phenyl core (45°) compared to the southeastern core (25°) may be less favorable for binding.

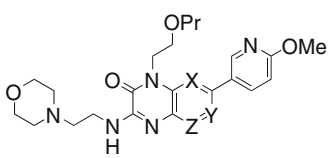
In an effort to further differentiate between the six core ring systems we collected information on metabolic stability, and, as

a measure of the compound propensity to interact with the hERG channel, dofetilide binding; the results from these studies are summarized in Table 3. None of the six prototype compounds significantly displaced dofetilide at 10 μ M. However, in keeping with expectations, the more lipophilic phenyl isomer, **2**, did show the most significant interaction (43%).⁶ In the case of southern pyridine **6**, 34% inhibition in the dofetilide competition assay translated into an IC₅₀ of 5.5 μ M in a hERG patch-clamp electrophysiology assay.

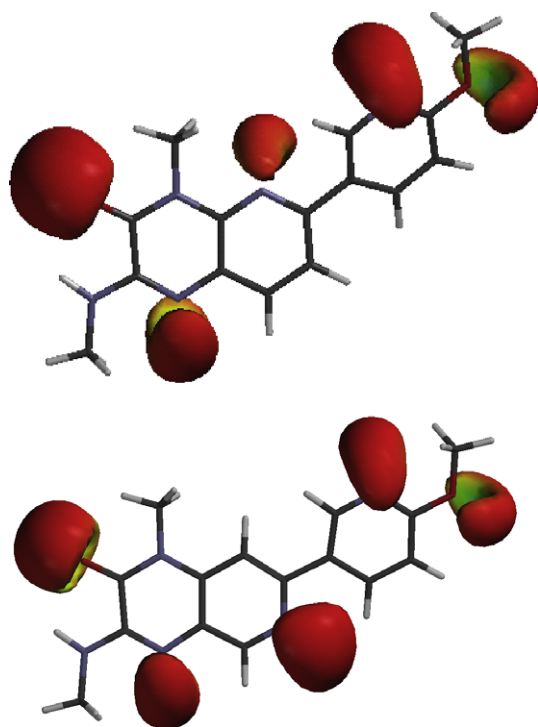
Consistent with our hypothesis that an increased biaryl twist would lead to improved solubility, we were also pleased to find that the southern pyridine analog, **6**, possessed significantly improved aqueous solubility of 46 μM at pH 7.4 compared to the more planar, pyridyl analogs such as: northern pyridine **1** (4.6 μM) and southeastern pyridine **5** (18 μM). For planar pyrimidine **3** we determined a solubility of 4.6 μM similar to that determined for **1**, highlighting the importance of log*D* modulation.

Table 2

PDE5, 6 and 11 potencies of the six pyrazinone isomers



Compound	X	Y	Z	PDE5 ^a	PDE6 ^b	PDE11 ^c
1	N	CH ₂	CH ₂	2.9	339	1540
2	CH ₂	CH ₂	CH ₂	0.9	177	>1990
3	N	N	CH ₂	1.21	83	1470
4	N	CH ₂	N	10.6	297	3560
5	CH ₂	N	CH ₂	0.07	11.3	346
6	CH ₂	CH ₂	N	0.34	61.8	1390

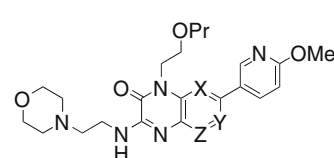
^a PDE5 IC₅₀ (nM).^b PDE6 IC₅₀ (nM).^c PDE11 IC₅₀ (nM).**Figure 2.** Comparison of the electrostatic potential of the Southeastern and Northern pyridines. Structures were optimized at HF/6-31G(d) and surface shown is the electrostatic potential colored on electron density (scaled at –20 kcal/mol).

All six compounds displayed modest and similar stability in human microsomal systems. Rat pharmacokinetic data,⁷ summarized in Table 4, is consistent with the in vitro metabolic stability data. Clearance values ranged from moderate to high and the bioavailability was moderate. Finally, the prototypes demonstrated moderate plasma protein binding.

The improved solubility and potency of southern pyridine **6** made it an attractive candidate to study in our acute, in vivo model of hypertension. Briefly, spontaneously hypertensive rats were IV-dosed with 1.5 mpk bolus of **6** and compound levels and blood-pressure were monitored over time.⁸ Encouragingly, this single dose of **6** resulted in a significant reduction (25 mmHg; baseline 190 mmHg to 165 mmHg) in blood-pressure for >3h. Compound levels at +3h, after which point the BP began to return to baseline levels, were approximately 7 × PDE5 IC₅₀.

Table 3

Dofetilide and metabolic stability of the six pyrazinone isomers



Compound	X	Y	Z	HLM ^a	Dof ^b
1	N	CH ₂	CH ₂	10	14
2	CH ₂	CH ₂	CH ₂	20*	43
3	N	N	CH ₂	22	15
4	N	CH ₂	N	12	11
5	CH ₂	N	CH ₂	38	23
6	CH ₂	CH ₂	N	18	34

^a Human Liver Microsomes % remaining after 30 min incubation.^b Dof: % inhibition at 10 μM.

* Hepatocytes.

Table 4Selected Pharmacokinetic parameters in rat (Sprague–Dawley)^a

Compound	V _d ^b	Cl ^c	T _{1/2} ^d	F (%)	ppb
1	8.0	67.6	3.1	23	89.6
4	5.2	151	0.6	ND	91.2
5	1.6	33.6	3.2	21	50
6	18.8	178	3.4	ND	76.5

^a IV: 2 mpk (n = 3) vehicle: 70% PEG400/20% 0.05 M citrate buffer/10% ethanol, pH 5; PO: 2 mpk (n = 3) vehicle: 0.5% methylcellulose/0.1% Tween 80 in 50 mM citric acid, pH 5.

^b L/kg.^c mL/min/kg.^d Hours.

In summary, we have described the design, synthesis and initial characterization of five novel sub-types of the pyridopyrazinone class of PDE5 inhibitors. In keeping with our hypotheses regarding key factors for binding, the southern and southeastern pyridyl isomers demonstrated a significant improvement in potency against PDE5. Both in vitro and in vivo measures of metabolic stability suggested that the six core ring systems behaved similarly and that further improvements in pharmacokinetic parameters would require optimization of the peripheral regions of the molecule. These studies will be the focus of subsequent reports.

References and notes

- (a) Beavo, J. A. *Physiol. Rev.* **1995**, 75, 725; (b) Corbin, J. D.; Francis, S. H. *J. Biol. Chem.* **1999**, 274, 13729; (c) Stamford, A. W. *Ann. Rep. Med. Chem.* **2002**, 37, 53.
- Owen, D.R.; Walker, J.K.; Jacobsen, E.J.; Freskos, J.N.; Hughes, R.O.; Brown, D.L.; Bell, A.S.; Brown, D.G.; Phillips, C.; Mischke, B.V.; Molyneaux, J.M.; Fobian, Y.F.; Heasley, S.E.; Moon, J.B.; Stallings, W.C.; Rogier, D.J.; Fox, D.A.; Plamer, M.J.; Ringer, T.; Rodriguez-Lens, M.; Cubbage, J.W.; Blevins, R.M.; Benson, A.G.; Acker, B.A.; Maddux, T.M.; Tollefson, M.B.; Bond, B.R.; MacInnes, A.; Yu, Y. *Bioorg. Med. Chem. Lett.* in press, doi: 10.1016/j.bmcl.2009.06.012.
- This structure has been deposited in the PDB under accession code 3HC8.
- Wang, W.; Hobza, P. *ChemPhysChem* **2008**, 9, 1003.
- The geometries on the core plus 4-methoxy-3-pyridyl were optimized at HF/6-31G* and frequencies were calculated to ensure the structures were minima on the energy surface.

Compound	Aryl–aryl twist (°)
1, 4, 5	25–28
2, 6	45–46
3	0

- Jamieson, C.; Moir, M. M.; Rankovic, Z.; Wishart, G. J. *Med. Chem.* **2006**, 49, 5029.

7. The Pfizer Institutional Animal Care and Use Committee reviewed and approved the animal use in these studies. The animal care and use program is fully accredited by the Association for Assessment and Accreditation of Laboratory Animal Care, International.
8. Briefly, SHR^s (Charles River Laboratories, Wilmington, MA) (14-weeks old, ~300 g) that were housed in a controlled environment (21 °C and 50% humidity) with a 12 h light–dark cycle and free access to standard rodent chow (Rodent 8640, HARLAN TEKLAD, Madison, WI) and water, were instrumented under anesthesia with bilateral jugular vein and right carotid artery catheters and allowed to recover for approximately 24 h prior to connection to the Culex[™] system. The Culex ABS system (Bioanalytical System) allows for continuous tethered BP monitoring, oral and intravenous administration of compounds and computerized blood sampling at multiple time points. Systemic arterial BP and HR were recorded continuously throughout the course of the study via a pressure transducer (Becton Dickinson, Sandy, Utah) connected to a data

acquisition system (ACQ-7700 digital amplifier and PONEMAH P3 Plus software) (Gould Instrument System, Valley View, OH). Compounds were formulated in 0.5% dimethyl sulphoxide (DMSO) (Sigma, St. Louis, MO) in 0.9% saline (Abbott Laboratories, North Chicago, IL). Following an equilibration period, baseline blood pressure (BP) and heart rate (HR) were monitored for 60 min prior to compound administration. At time zero each of four animals per study received a 1.5 mg/kg intravenous bolus dose of compound and monitored for a further 6 h. Whole blood (150 µl) was automatically sampled via the right jugular catheter at 15, 30, 60, 180 and 360 min following compound administration for plasma concentration analysis of compound. Blood was stored in capped, refrigerated vials (4 °C) containing sodium heparin (Bioanalytical System, Inc.). Plasma was separated by centrifugation at 3000 rpm for 10 min at 4 °C and then stored at –80 °C. Plasma sample compound concentration analysis was performed using an LS/MS/MS triple quadrupole mass spectrometry system (Siex–API 4000).